NASA TECHNICAL NOTE

NASA TN D-3211

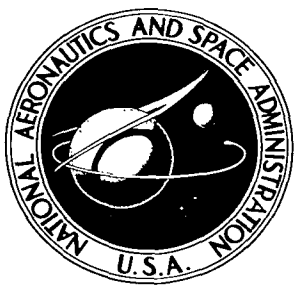

A DOUBLE-FOCUSING MAGNETIC MASS SPECTROMETER FOR SATELLITE USE

by
Carl A. Reber

Goddard Space Flight Center
Greenbelt, Md.
and
Lawrence G. Hall
Consolidated Systems Corporation
Pomona, Calif.

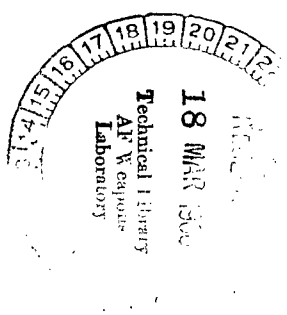

NATIONAL AERONAUTICS AND SPACE ADMINISTRATION • WASHINGTON, D. C. • MARCH 1966

NASA TN D-3211

A DOUBLE-FOCUSING MAGNETIC MASS SPECTROMETER FOR SATELLITE USE

By Carl A. Reber

Goddard Space Flight Center
Greenbelt, Md.

and

Lawrence G. Hall

Consolidated Systems Corporation
Pomona, Calif.

NATIONAL AERONAUTICS AND SPACE ADMINISTRATION

For sale by the Clearinghouse for Federal Scientific and Technical Information
Springfield, Virginia 22151 – Price $1.00

ABSTRACT

The requirements, configuration and characteristics of the mass spectrometer system used in the Explorer XVII satellite are described. The double-focusing (angle and energy) magnetic instrument ionizes neutral species, collects the ions of He^+, N^+, O^+, H_2O^+, N_2^+ and O_2^+ in fixed position collectors, and commutates resulting currents into a logarithmic detector system. Sequential measurements of the six ion currents over a compressed seven-decade dynamic range are provided. The open ion source extends from the satellite surface to allow entry of the 0.4 to 12 ev neutral particles from 2π steradians solid angle. Sensitivity for m/e 28 of N_2 is typically 10^{-4} amperes/torr when the ion source potentials are adjusted for acceptance of energetic particles. Flat-topped peaks are used to minimize error due to possible drift in the high voltage power supplies. A 360°C bakeout and ceramic-sealed caps, which permit launching in vacuum and are ejected in flight, reduce the background due to outgassing.

CONTENTS

Abstract ii

INTRODUCTION. 1

DESIGN PHILOSOPHY 2

TUBE DESIGN. 3

- Ion Source. 3
- Ion Lens 5
- Analyzer. 7
- Break-off Hat 11

DETECTOR SYSTEM AND ELECTRONICS 11

- Electrometer Amplifier. 11
- Logarithmic Amplifier and In-flight Calibrator 13
- Logic System. 14
- Electron Beam Control and Monitor. 14
- Power Supplies 15

SYSTEM PERFORMANCE 15

- Environmental Testing 15
- Calibration 16
- Flight. 16

ACKNOWLEDGMENTS 16

References 16

A DOUBLE-FOCUSING MAGNETIC MASS SPECTROMETER FOR SATELLITE USE

by
Carl A. Reber
Goddard Space Flight Center

and

Lawrence G. Hall
Consolidated Systems Corporation

INTRODUCTION

Study of the earth's upper atmosphere by direct measurement techniques has been a realizable and productive possibility since shortly after World War II. Early endeavors were hampered by the lack of knowledge of the environment and the state-of-the-art of vacuum techniques at the time, but as the demand increased for more knowledge in this region of the atmosphere, the techniques and the instrumentation employed gradually became more sophisticated. In 1953, a mass spectrometer (Reference 1) was first successfully flown on a rocket to measure the composition of the atmosphere above 90 km. Since then, mass spectrometers have been flown many times from a number of locations.

The purpose of this paper is to describe the neutral gas mass spectrometer instrumentation of the Explorer XVII satellite (1963 09A) launched in April, 1963. The two essentially identical spectrometers flown were designed specifically for satellite flight and thus the following problems were considered: (1) reduction of spectrometer and satellite background gas pressure to a small value; (2) measurement of atomic species with minimal surface interaction; (3) the effect of relatively high initial ion energies due to satellite velocity and (4) geometry of the spectrometers and their location.

The measurement conditions were particularly enhanced with the Explorer XVII satellite which was conceived specifically for upper atmosphere studies and embodied state-of-the-art vacuum techniques in its design and construction. The satellite, shown in Figure 1, is a battery operated, spin stabilized, vacuum tight sphere with all the gages mounted flush with the surface so that no line of sight existed between any vacuum sensor and any other portion of the satellite. Outgassing, recombination and other surface effects arising from the large area of the satellite thus had a minimum influence on the gage measurements. The other experiments on the satellite include Bayard-Alpert and Redhead type pressure gages and electrostatic probes to measure ion densities and electron energies.

DESIGN PHILOSOPHY*

The launch and orbital environment of the mass spectrometer defined many of the guidelines for its design. Foremost among these were reliability and stability, as the spectrometer was to be prepared and calibrated on the ground and then required to operate unattended for a number of months following launch.

The 250-km perigee and 925-km apogee of the satellite would expose the mass spectrometer to an estimated ambient pressure range of 10^{-5} torr to 10^{-11} torr. Previous spectrometer measurements at lower altitudes indicated that the predominant gases to be encountered throughout the orbit would be nitrogen and oxygen. The objective of the Explorer XVII experiment was thus to obtain more precise density measurements for these gases, plus helium, in addition to more comprehensive coverage to help define altitude, geographic, diurnal and seasonal variations.

As the average thermal velocity of the ambient particles is small compared to satellite velocities of approximately 8 km/sec, their velocity relative to the spectrometer is almost the (nearly constant) satellite velocity. Thus, their apparent kinetic energy, $mv^2/2$, is essentially proportional to their mass. For molecular oxygen, the heaviest mass being sampled, this energy is approximately 12 electron volts. Further, since the mass spectrometers were to be located on the spin axis, which could be considered as fixed in direction throughout one orbit, the relative velocity vector (Figure 2) of the incoming particles would rotate over a complete 2π-steradian solid angle for each spectrometer. The "nude" type ion source was

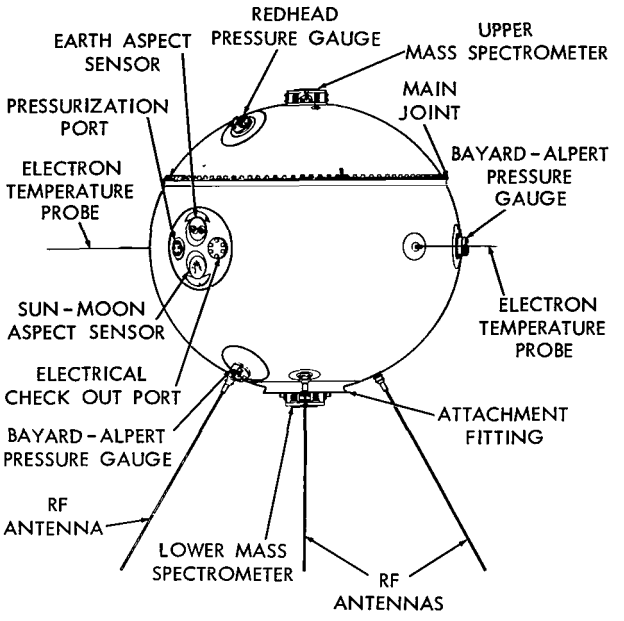

Figure 1—The Explorer XVII atmospheric structure satellite, showing the location of the various sensors.

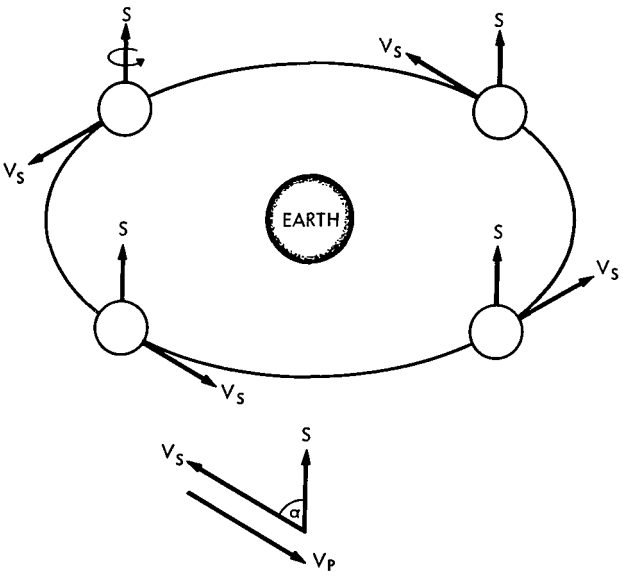

Figure 2—The relationship between the satellite spin axis, S, which is a very slowly varying function of time, and the satellite velocity vector, V_s.

*Meadows, E. B. "Design Requirements of a Mass Spectrometer for Satellite Use," presented at 8th Annual Meeting of ASTM Committee E-14 on Mass Spectroscopy, Atlantic City (1960) (Unpublished).

designed to utilize an orthogonal orientation of the velocity vector and the gage axis to minimize the surface interactions of the ambient particles before they are measured. Thus, for this type of ion source the minimum disturbance of the atmosphere occurs in this condition. As the orientation approaches direct ram, surface phenomena gradually become of greater importance.

The requirements to focus multi-directional particles in a range of energies up to 12 ev while maintaining high sensitivity dictate not only an unusual ion source but also an analyzer of particular characteristics. These include: (1) a large solid angle of acceptance, (2) a short ion path length and, (3) a large tolerance to forward energy variation.

In order to accept these large energies and angles a double-focusing instrument is necessary. Furthermore, since the energy of the incoming particle increases linearly with mass, it is essential that the forward accelerating voltage not be reduced at high mass as required in a voltage scanned magnetic instrument. Berry (Reference 2) has shown that voltage scanning with thermal particles of 0.025 ev energy can introduce discrimination; at 12 ev the effect would be considerably more severe. Consequently, to meet the requirement of fixed accelerating voltage, a spectrograph type instrument is used where the ions are dispersed along a focal plane and where both electric and magnetic fields remain constant.

For the gases of interest in this experiment, six ion collectors are positioned along the focal plane and the prechosen masses sampled in sequence by a switching arrangement in the amplifier. Provision is also made to periodically sample the total ion current entering the analyzer region. Since the amplifier monitors a DC level during the sampling period a longer time constant and lower noise design can be used than if the spectra were scanned. A further improvement in signal to noise ratio appears possible in future experiments by providing an amplifier for continuous monitoring at each mass position of interest.

TUBE DESIGN

The mass spectrometer* (Figures 3 and 4) is a tandem double-focusing instrument with a 60° electric sector and a 90° magnetic sector. Among the features of the tube which make it particularly useful for measurements from a satellite are the ion source and electrostatic lens which precede the mass analyzer. The tube itself is normally evacuated prior to and during launch, the outer cover, or "break-off hat", being ejected once a region of suitably low pressure has been reached.

Ion Source

The ion source is basically a cylindrically symmetric design. Exceptions are the electron beam system, ion source exit slit and a "wedge lens" (to be described). A cross section of the ion

*Hall, L. G., Howden, P. F., and Iwasaki, T. F., "Design of a Mass Spectrometer for Use in a Satellite", presented at 8th Annual Meeting of ASTM Committee E-14 on Mass Spectroscopy, Atlantic City (1960) (Unpublished).

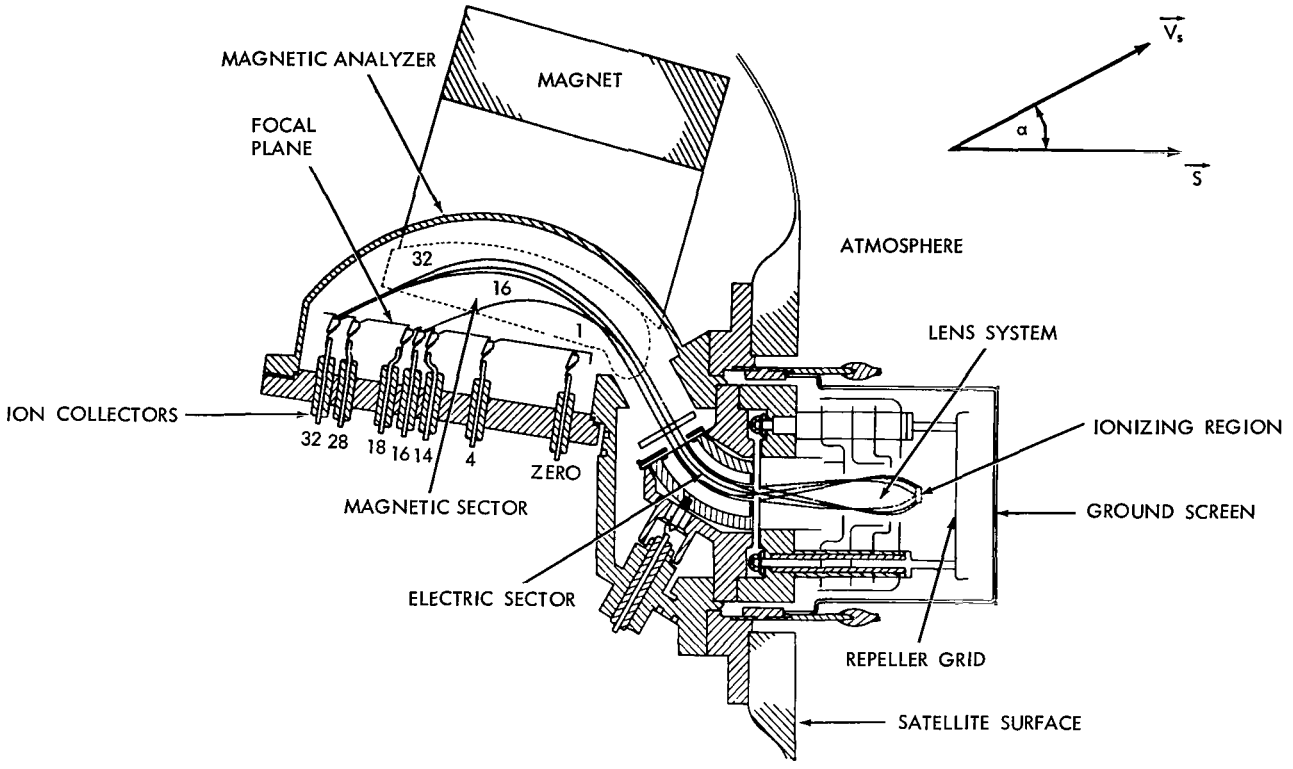

Figure 3—The mass spectrometer cross section in the x-y plane.

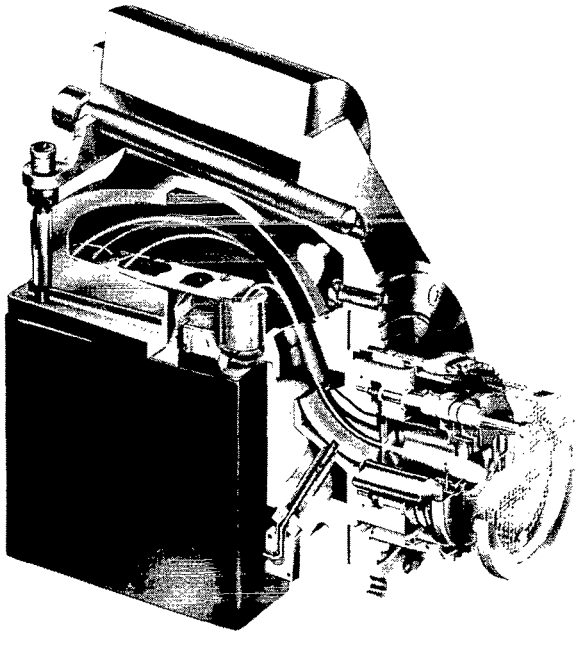

Figure 4—Mass spectrometer perspective cutaway showing magnet mounting and the amplifier attachment to the collector flange.

source giving pertinent dimensions and the typical voltages used is shown in Figure 5. Also shown in light lines are the equipotentials in a plane of symmetry, and in dashed lines, the electron beam. The principal construction materials are tantalum for the ion lenses, stainless steel for the repeller and base flange and aluminum oxide ceramic for the insulators.

A pair of 0.4375 inch diameter Alnico magnets mounted in a magnetic stainless steel base ring form a "C" magnet which creates the field for the alignment of the electron beam. The electrons are emitted from a 0.007 inch rhenium wire filament located adjacent to one pole and are accelerated to 45 ev in passing through the accelerator electrode. Back emission is prevented by connecting the shield to the negative side of the DC heated filament. A filament current of 3.2 amperes from a 3.1-volt battery source produces the nominal 500 μA ionizing

current. Of this, 470-480 μamps reach the anode, the remainder going to other electrodes.

The general path of the beam is an arc extending above the accelerator electrode to the anode aperture. The constraining magnetic field strength is nominally 1000 gauss at the filament and anode and 200 gauss at the peak position of the beam 5.5 mm above the surface of the accelerator. The electron energy increases to 70 ± 15 ev at the peak position and passes through an electric field in this region of 210 volts/cm. The electron beam thickness is calculated to be 1.4 mm, due both to the divergence of the magnetic field and the cycloidal motion of the electrons in the crossed fields. Calculated values of electron beam position, energy and energy spread are obtained from ion suppression curves measured with a faraday cage beyond the source slit and from the equipotential plot. The width of the electron beam as measured by the deposit on an interceptor plate is 7 mm.

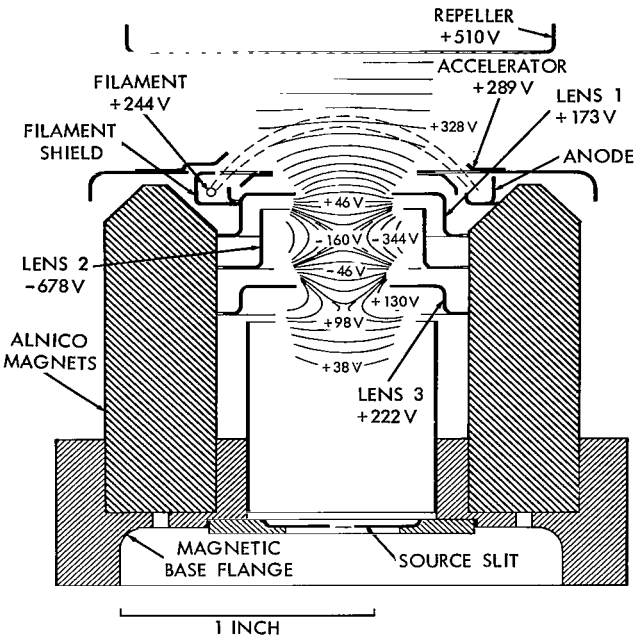

Figure 5—Ion source cross section. Equipotentials are shown for the typical voltage settings as indicated.

Calculations of the electron cycloidal "fine" motion in the crossed E and B fields given above, assuming no initial energy, indicate that the electron completes one cycloidal loop of 0.6 mm height and 1.85 mm side motion in traversing a forward distance of 8.8 mm. Consequently the envelope of group motion of a ribbon beam of electrons, as illustrated in Figure 3, is at an angle of 12° to a symmetry plane which includes the axes of the magnets. For this reason the electron beam and magnets are rotated with respect to the source slit.

Since the repeller is at a potential of approximately +500 volts with respect to the satellite, large numbers of ionospheric electrons would be attracted, with a resultant change in the potential of the satellite relative to its surroundings. As this change in potential could conceivably compromise other experiments aboard the satellite, the exposed portion of the spectrometer is surrounded by a grid electrically connected to the skin of the satellite. The effectiveness of this grid has been demonstrated by flight data from the electrostatic probe experiment which show no apparent change in satellite potential whether the spectrometer is operating or not. Studies are being carried out to determine if the grid can be removed on subsequent flights without affecting the spacecraft potential. Both the grid and the repeller have an optical transparency of about 0.80.

Ion Lens

The desired characteristics of the ion lens system are that it (1) focuses particles in such a manner as to be independent of the energy up to some relatively high limiting value and (2) provides upper

bounds for angles and energies of transmitted particles which are acceptable for proper resolution in the analyzer. These requirements can, in principle, be made mutually compatible.

The first characteristic can be obtained approximately when an image of the ion "object" created at the electron beam is formed at the source exit slit. The nature of a perfect image-to-object relationship requires that all "rays" passing through a point in the object plane also pass through a related point in the image plane, within the limits of acceptance of the transmission system. In the case of charged particles, an angle of incidence of 90° for an ion having considerable initial energy may be within the limits of acceptance of the transmission system providing the object plane is in an axial field. The quality of the image is, however, affected by imperfections of the lens system and by the typical forward velocity aberration of electrostatic lenses (Reference 4).

The angle can be bounded by the application of Abbe's law (Reference 4, page 12) which states for an image-object relationship:

$$y_1 V_1^{1/2} \sin\theta_1 = y_2 V_2^{1/2} \sin\theta_2 \quad , \tag{1}$$

where subscripts 1 and 2 refer to conditions at the object and image planes respectively; y = distance from the axis; qV = particle kinetic energy; θ = angle of incidence; and q is the charge on the particle. Since $y_2/y_1 = M$ = magnification, and, if we assume the worst case, is $\theta = 90°$, then

$$\sin\theta_2 = \frac{1}{M}\left(\frac{V_1}{V_2}\right)^{1/2} \tag{2}$$

includes the most divergent particles. If no fields exist at the exit slit, then for small angles we can take the emergent half angle α equal to $\sin\theta_2$, or

$$\alpha = \frac{1}{M}\left(\frac{V_1}{V_2}\right)^{1/2} . \tag{3}$$

It is clear that scanning the instrument by reducing V_2 would increase the angle, or, in this instance, reduce the upper limit of acceptable energy and cause discrimination against higher masses.

It is shown later that an angle of 0.09 radians is acceptable for the resolution required. The most energetic particle to be focused is O_2 at 12 ev with the mean ion exit energy of 330 ev. Therefore, $M \approx 2.1$ to obtain the desired limiting angle. It is seen that the exit angle can be bounded by the method above. However, the forward energy spread is not greatly altered and therefore the analyzer must be capable of accepting a range of approximately 40 ev due to combined initial energies and voltage range of the electron beam.

It may be noted in Figure 3 that lens 3 is unsymmetrical in that a short cylindrical section extends toward the base flange on one side. This section is 120° in angular extent, 4.7 mm long and symmetrically centered 90° to the plane of the magnets. The purpose of this tab is to correct for

deflection of the ion beams in the source magnetic field by means of a single potential "wedge" lens. When the "wedge" lens is placed at a positive potential some separation of m/e 4 and m/e 28 still occurs; however, the separation is less than that expected with no correction.

In order to establish more accurately the focusing characteristics of the ion source, further investigation is being conducted with an electrolytic tank trajectory plotter and a three-dimensional model. The results of this investigation on energetic particles will be incorporated into calculations of the relationship between the measured and ambient number densities.

Analyzer

The analyzer was selected from a number of double-focusing mass spectrographs comprehensively examined and described by Hintenberger and König (Reference 3). Several particular properties necessary for the required measurements were: (1) large aspect ratio (solid angle of acceptance), (2) short ion path length (i.e., compactness) and (3) small aberration coefficients over a wide mass range.

The instrument size is based on a characteristic magnetic radius of $r_m = 5$ cm for the heaviest mass to be investigated (m/e 32). The ion beam enters through the object slit (source exit slit) of width, $S_0 = 0.4$ mm located 0.15 cm from the entrance of an electric sector having a radius $V_e = 2.4$ cm. The 60° electric sector is terminated with a Z axis einzel lens (Reference 4) for focusing in a direction parallel to the magnetic field and the termination is located 2.65 cm from the theoretical entry point of the magnetic field. A Herzog shunt (Reference 5) helps to establish a definable entrance boundary to the magnet, while the Armco iron electric sector elements shunt the field to a negligible value in the electric sector region.

The magnet is a "C"-shaped Alnico V magnet having a gap of 1.6 cm with pole pieces shaped as shown in Figure 6; this geometry provides 90° deflection of all beams. Due to the large magnet gap, the region of the magnetic field is not of simple bounded form, as can be seen in the central plane field plot, and consequently ray-tracing techniques are required to establish the ion paths.

In such a system the ion position at the focal plane can be expressed as a power series in α_e and β where α_e is the half-angle of entry and $\beta = \pm\Delta v/v$ where v is the velocity and Δv the deviation in velocity from the central value. Consequently, $\beta = \pm\Delta V/2V_1$ where qV_1 is the injection energy. The general form of the series through second order is, in the notation of Hintenberger and König (Reference 3):

$$y_B = r_m \left(B_1 \alpha_e + B_2 \beta + B_{11} \alpha_e^2 + B_{12} \alpha_e \beta + B_{22} \beta^2\right) \quad , \tag{4}$$

where y_B is the displacement from the central ion path. As defined by them, for a mass spectrograph, the coefficients B_1 and B_2 are zero at all points along the focal plane. Also for the idealized form of this configuration $B_{12} = B_{22} = 0$ and $B_{11} = 0.86$. It is seen that the displacement, y_B, is

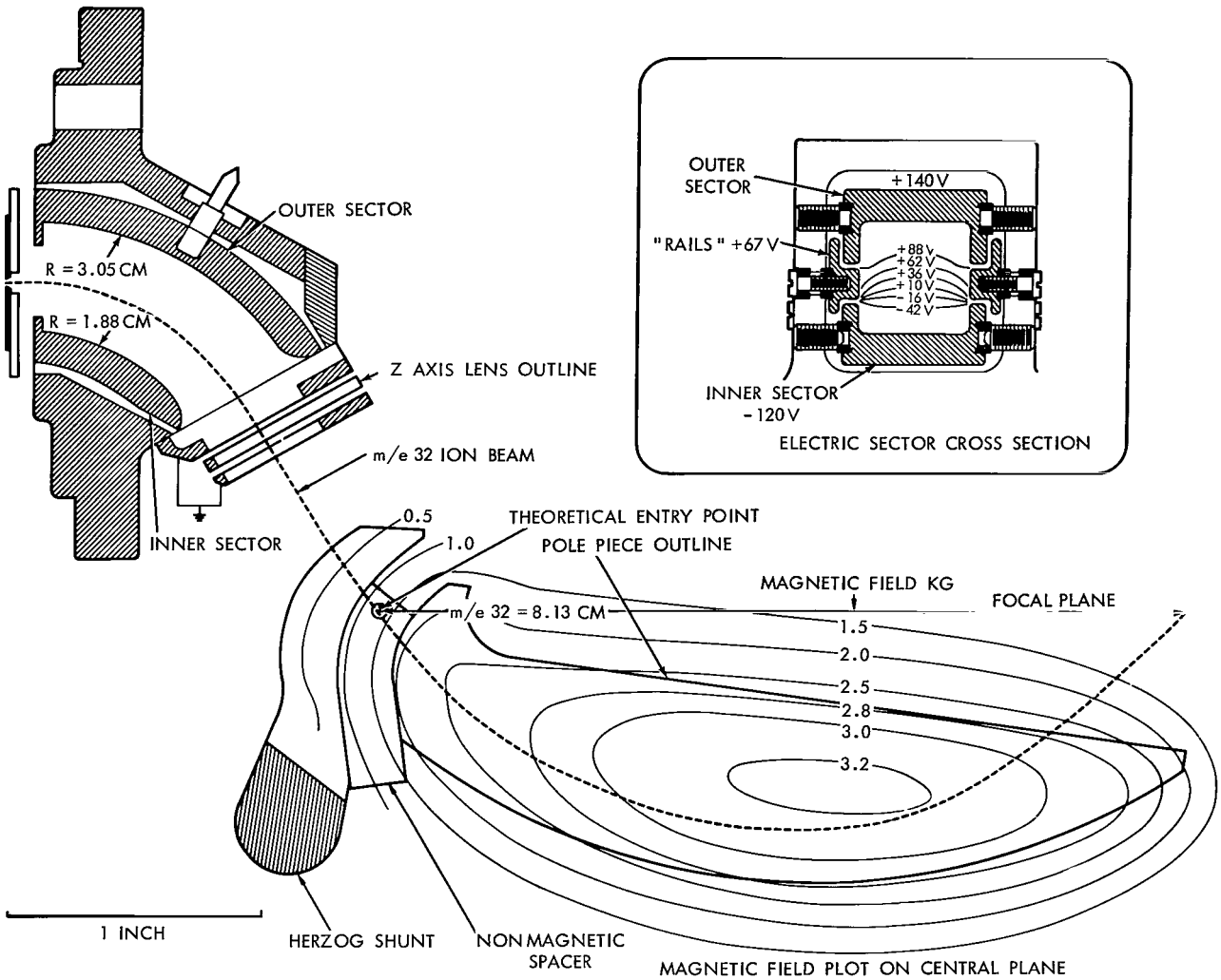

Figure 6—Electric sector and magnet configuration.

thus independent of the sign of α_e. In order to obtain the image size, the magnified object size must be added to the aberration. The magnification was determined from ray tracing to be 1.8. Thus, the theoretical image size measured in a plane perpendicular to the ion beam becomes

$$S_I = M S_0 + B_{11} r_m \alpha_e^2 = 1.8 S_0 + 0.86 r_m \alpha_e^2 \quad . \tag{5}$$

When projected onto the focal plane, both the image size and dispersion are multiplied by sec γ where $\gamma = 52°$ is the angle between the ion beam direction and the normal to the focal plane.

The dispersion between two ion beams perpendicular to their path is given in this case by $D = r_m(\Delta m/2m)$ where m is the mass and Δm, the difference in mass. Thus, the dispersion between

m/e 28 and m/e 32 based on m = 30 is D = 0.3222 cm, while from Equation 5 the theoretical image size for α_e = 0.09 rad. and S_0 = 0.04 cm, is S_I = 0.107 cm.

An important consideration in the design of an instrument for continuous, unattended space flight is that wide temperature and voltage variations are probable. Consequently, the collector slits are made large enough (e.g., S_R (m/e 32) = 0.285 cm and S_R (m/e 28) = 0.315 cm) to accommodate relatively large variations in beam position without change in collected current. From the image size given above and the projected resolving slit size, the theoretical resolving power is m/Δm = 11.7 in region of mass 30 for 2% valley height between peaks. Other resolving slits are adjusted in size to suit the nature of the separation requirements, such as eliminating OH^+ due to water background from the O^+ collector.

An example of the resolution obtained from m/e 28 and 32 (air) and m/e 4 (He) under the conditions above is shown in Figure 7. The peak top is sufficiently broad that for N_2 the voltage supply can vary by ±4% before reducing the ion current by 2%. Helium, at the low end of the scale, is even more tolerant of voltage change. The values of the main voltage supplies are monitored by telemetry with an accuracy of better than 0.5%.

While the original calculations were based on a cylindrical condenser type electric sector, improved performance was found to occur experimentally when operated as a toroidal condenser. Figure 6 also illustrates a cross section of the electric sector and indicates typical potentials. In order to reduce the physical extent of the condenser in the Z direction, a pair of "rail" electrodes terminate the ±Z boundaries (Reference 6). When the "rails" are operated at zero potential, a cylindrical condenser is produced, or, when operated at a positive potential, as shown, they produce an approximate but adjustable toroidal field.

As a result of the toroidal field an effective Z constraining force is added to the system. In addition to the Z axis lens, focusing is produced at the entrance to the magnetic field when, as shown by Herzog (References 7 and 8), the non-normal entrance in the x-y plane produces a convergent lens action in the Z direction having a focal length of $r_m/\tan\epsilon' = 12.2$ cm. $\epsilon' = 22.2°$ is the mean angle of the ion beam to the normal of the magnetic field at the entrance. The path length from magnet entry to collector for

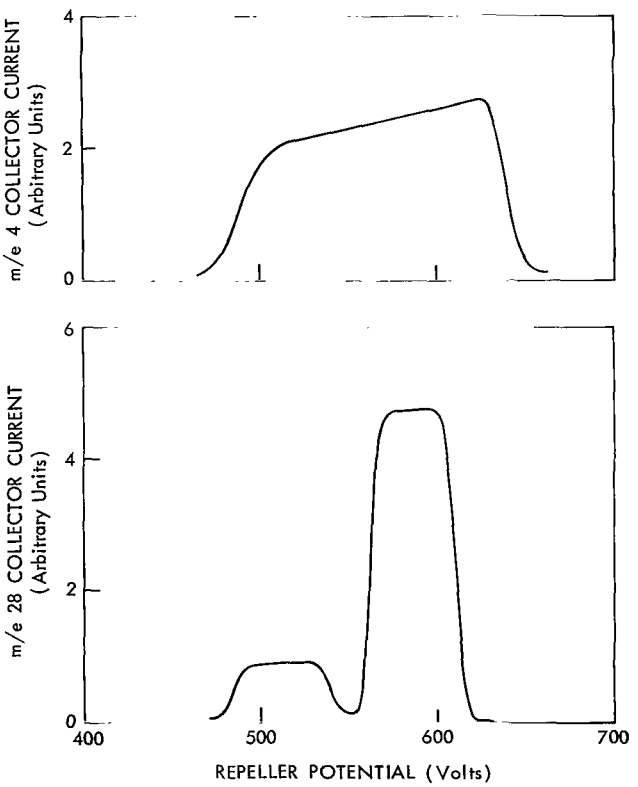

Figure 7—Peak height of m/e 32 and 28 on the m/e 28 collector and peak height of m/e 4 on the m/e 4 collector as a function of the high voltage divider string potential referenced to the repeller.

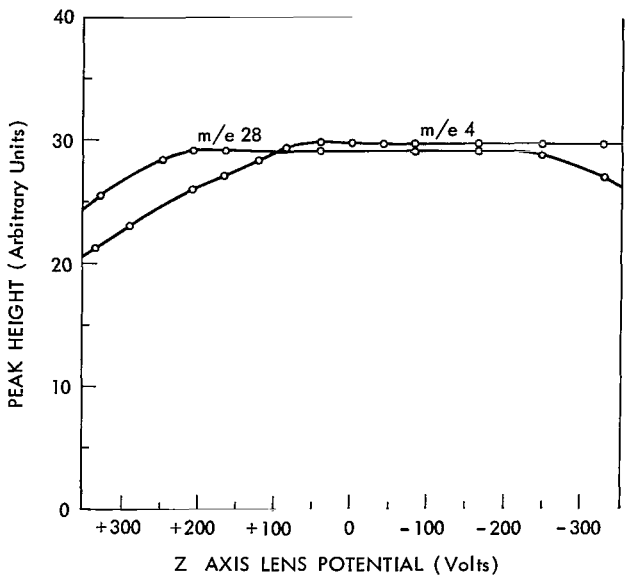

Figure 8—Peak height of m/e 28 (N_2) and m/e 4 (H_e) versus Z axis lens potential.

r_m = 5 cm is 9.3 cm, or approaching that required for Z focus at the collector.

From an initially divergent beam the resultant Z focusing produces a slightly convergent beam between sectors due to the toroidal field and Z lens and additional convergent focusing at the magnet entrance for a "focal point" at the collector. Under these conditions the Z lens can be varied over a wide range of voltage, as shown in Figure 8, before the image is defocused beyond the 1.0 cm slit length at the collector. This condition implies that 100% of the ion beam entering the analyzer can be collected at appropriately placed collectors. A direct confirmation of 100% collection was made by comparing the summation of ion currents to the collectors against the undeflected current collected on the outer electric sector and they were found to agree with an experimental error of 2%. An in-flight measurement of total ion current is made based upon this condition.

Once each sampling cycle the negative electric sector and neighboring electrodes are switched to ground potential and the positive sector is switched to the input of the electrometer amplifier. In this mode of operation the mass spectrometer becomes an ionization pressure gage, measuring the total ion current entering the analyzer. This serves both as a check on the focus of the analyzing region and as a check on the choice of gases being monitored on the individual mass collectors. A discrepancy between the total ion current and the sum of the individual ion currents could indicate the presence of an unmonitored gas.

The sensitivity to N_2 at m/e 28 is typically 10^{-4} amperes/torr (at a total electron emission of 500 μa) when the ion source potentials are adjusted for acceptance of energetic particles. If the ion source is adjusted for maximum sensitivity a value of greater than 10^{-3} amperes/torr is obtained, which is calculated to be 0.4 of that due to the theoretical ionization in the projected area of the accelerator aperture.

Other gases investigated on Explorer XVII in addition to helium, molecular nitrogen, and molecular oxygen, are atomic nitrogen, m/e 14; atomic oxygen, m/e 16; and water vapor, m/e 18. Water vapor, while not expected to be a significant part of the ambient atmosphere above 250 km, is expected to be present from surface outgassing. When dissociated in the source the water vapor contributes to ion currents of mass 16. Outgassing contributions to the background are recognizable in a given spectrometer when it is looking "back" into the wake of the satellite. At these times, because of their relatively low thermal velocity, a negligible fraction of the ambient particles is able to overtake and enter the source region.

Break-off Hat

In order to maintain low pressures in the tube prior to launch, both for purposes of operation and to keep the tube free from contamination, it is closed off by a metal-ceramic-metal seal hat-like cover (Figure 9). Once orbit is attained, teflon sealed pyrotechnic chisels break the ceramic, and springs eject the hat and the break-off mechanism. The source has been designed so that once the hat is removed the ionizing region "sees" no surface that has not been thoroughly baked in a vacuum. That is, there is no line of sight between the sampling volume and any part of the satellite. (In the case of the bottom spectrometer on Explorer XVII this is not rigorously true, as there is a small solid angle subtended at the source by the antennas. The total solid angle involved is quite small, however.)

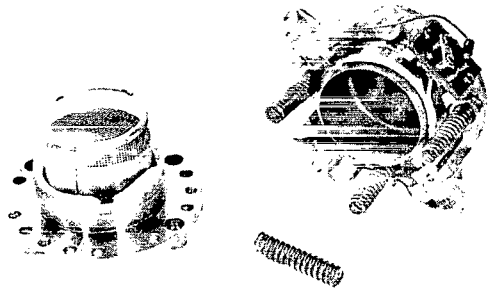

Figure 9—The break-off hat showing the part that remains on the spectrometer to the left and the part that is ejected on the right.

DETECTOR SYSTEM AND ELECTRONICS

A two amplifier detector system (Figures 10 and 11) is employed to fulfill the rather diverse requirements of large dynamic range, low current detection and maximum accuracy.

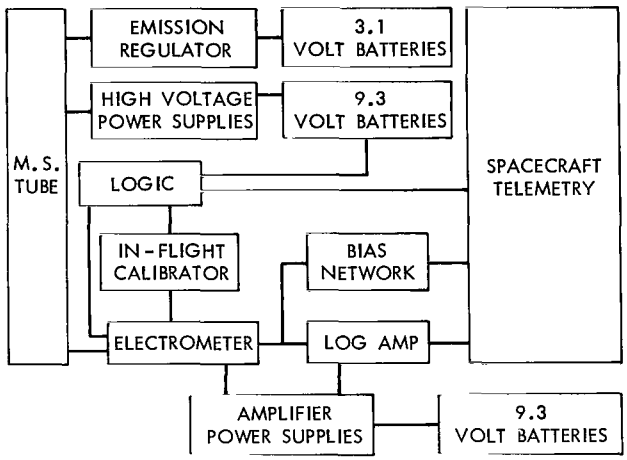

Figure 10—Block diagram of the mass spectrometer system.

A sensitive electrometer amplifier is used to detect the low currents incident on the various ion collectors. The output signal of the electrometer, with a dynamic range of nearly five decades, is fed into a logarithmic amplifier, the output of which is zero to five volts to match telemetry. Periodically, an in-flight calibration is introduced to minimize errors in the system.

Electrometer Amplifier

The electrometer amplifier is mounted directly onto the collector flange of the mass spectrometer (Figure 12). Situated between the individual ion collectors and the input to the electrometer tube is a set of glass reed switches* which performs the function of routing the ion current incident on a selected collector into the electrometer and shorting the other collectors to ground

*Type MRG-15 mfd. by Hamlin, Inc., Lake Mills, Wisc.

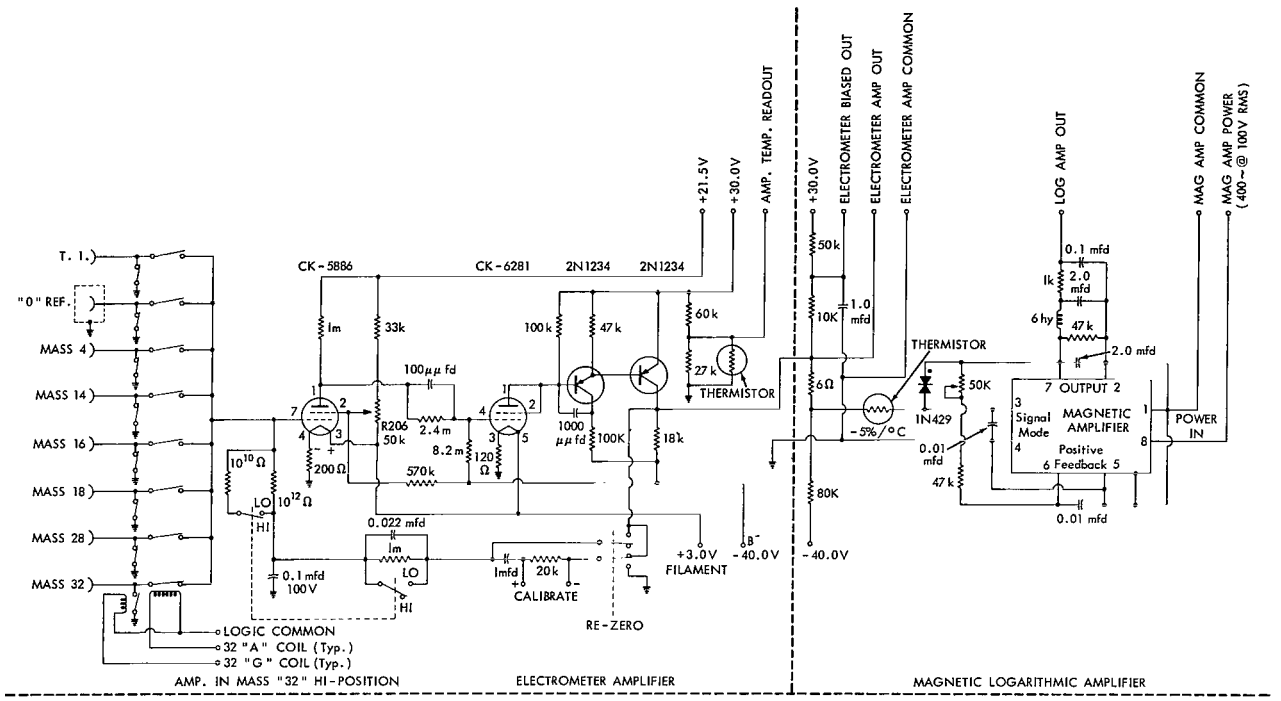

Figure 11—Schematic of the detector system.

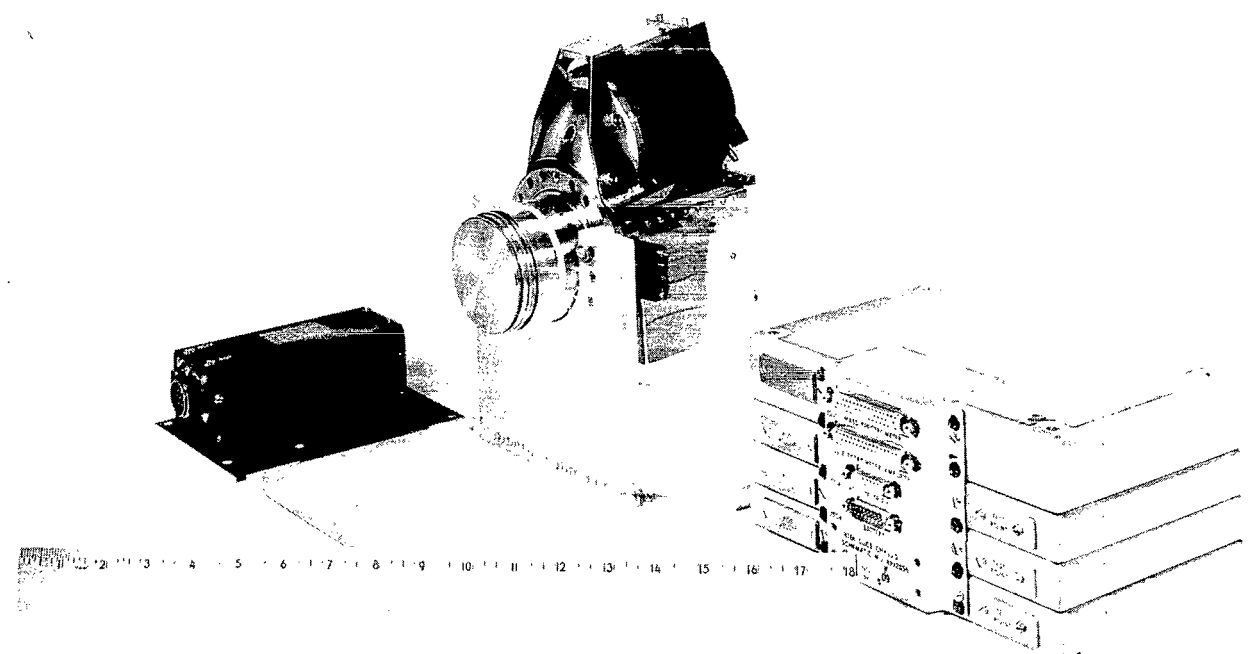

Figure 12—Photograph of the components of the mass spectrometer system.

to prevent charge buildup. To achieve the desired dynamic range, two input resistors are used: a 10^{10}-ohm resistor provides the low sensitivity performance and a 10^{12} or a 10^{13}-ohm resistor is used for high sensitivity. In practice, the 10^{10}-ohm resistor is switched in parallel with the other resistor for the low sensitivity range.

The amplifier uses a carefully selected and processed CK 5886 electrometer tube on the input and utilizes unity negative feedback. The minimum detectable signal level is 0.2 millivolt using the 10^{12}-ohm resistor. This sensitivity is a result of 1) using four seconds for observation of a given current, which allows a long time constant for the logarithmic amplifier and 2) an automatic zeroing feature. The saturation voltage of the amplifier is approximately 20 volts, corresponding to 2×10^{-9} amperes ion current in the low sensitivity mode.

The drift is normally less than 0.2 mv/min in the low sensitivity position and 0.5 mv/min in the high sensitivity position. DC drift problems are reduced by a rezeroing arrangement which once a minute samples the deviation from zero at the output with no input signal, automatically inverts this error signal and inserts it into the feedback loop. Also, the collector with the lowest expected ion current, helium, is sampled immediately after this rezeroing operation so there will have been a minimum amount of drift at this time. This approach is carried through the sequence, with the largest anticipated signal being sampled last. Amplifier warm-up time after turn-on is nominally 15 seconds to be within 1 mv of the stable zero.

Logarithmic Amplifier and In-flight Calibrator

The usable signal level out of the electrometer amplifier ranges from less than a millivolt to more than 20 volts. The associated pulse code modulation telemetry system can resolve 25 millivolts and saturates at about six volts; therefore a logarithmic amplifier is used to interface the two units. Along with the necessary attributes of voltage gain and range compression, the log amplifier has another, less obvious advantage. In contrast to the linear read-out device, which has a reading accuracy dependent upon the level of the signal being monitored, the log amplifier exhibits a nearly constant reading accuracy, the actual error being only a function of the slope of the logarithmic curve. The log amplifier (Figure 11) used with the mass spectrometer possesses an average error factor of about 8.5, i.e., a resolution of 1.0% (of full scale) in reading the output of the log amplifier appears as an 8.5% (of signal) resolution in the input current.

The logarithmic relationship is obtained by first converting the electrometer amplifier output voltage to a current source. This source then provides the input current for a closed loop magnetic amplifier* having a 1N429 double anode zener diode as the feedback element. The characteristics (Reference 9) of this diode produce an approximately logarithmic current relationship (Figure 13). Due to the temperature sensitivity of the log diode it is necessary to use a temperature compensating thermistor in the current source circuit.

As the major critical components of the log amplifier remain somewhat temperature-sensitive it was considered advantageous to employ an in-flight voltage calibrator. This consists of a seven

*Type M-5527 mfd. by Airpax Corp., Fort Lauderdale, Fla.

step voltage staircase which is inserted periodically into the feedback loop of the electrometer amplifier and which appears as nearly equidistant steps on the output of the log amplifier. Thus, the appropriate calibration curve can be constructed whenever the satellite is interrogated in orbit. In addition, the temperature of the resistors in the electrometer amplifier is telemetered so the temperature coefficient of these elements can be considered in data analysis.

A second, independent check on the log amplifier is supplied by a biased, linear readout of the electrometer voltage (See Figure 11). By utilizing a biasing network and voltage divider, the first six volt range of the amplifier provides a 0 to 5 volt signal for telemetry. Thus, additional calibration points are obtained in this range as well as an increased reading accuracy of 0.5% for signals near six volts.

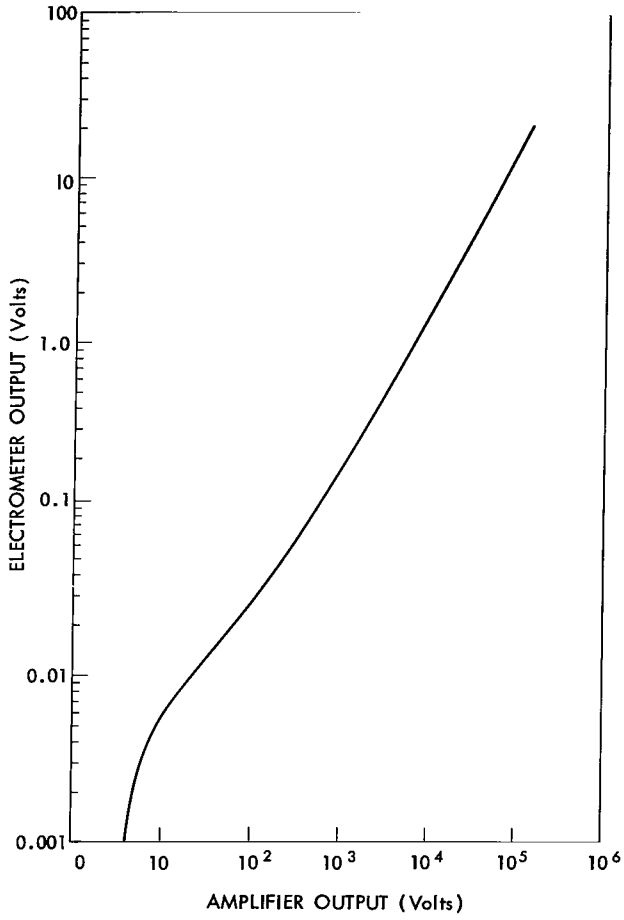

Figure 13—A typical response curve of the logarithmic amplifier.

Logic System

The sequencing and selection of the masses to be monitored is controlled by a solid state matrix which uses a neon bulb relaxation oscillator as a clock. A voltage staircase "mass marker" is also generated to indicate the state of the logic and mass position at any instant of time (Figure 14). The sample mode occurs at the beginning of the cycle, at which time the electrometer rezero network samples the deviation from zero voltage. In the zero position the zero signal level of the amplifier is monitored in both the low and high sensitivity conditions. The nominal time constant per step of four seconds is dictated by detector noise consideration and the high sensitivity required. The normal operating time in orbit is three minutes per turn-on.

Electron Beam Control and Monitor

A regulator is employed to sense the total electron current being emitted by the mass spectrometer filament and maintain the preset level to within a 1% tolerance. One subcommutated telemetry channel is devoted to a DC-DC converter which monitors the emission current and the acceleration voltage of the ionizing electrons.

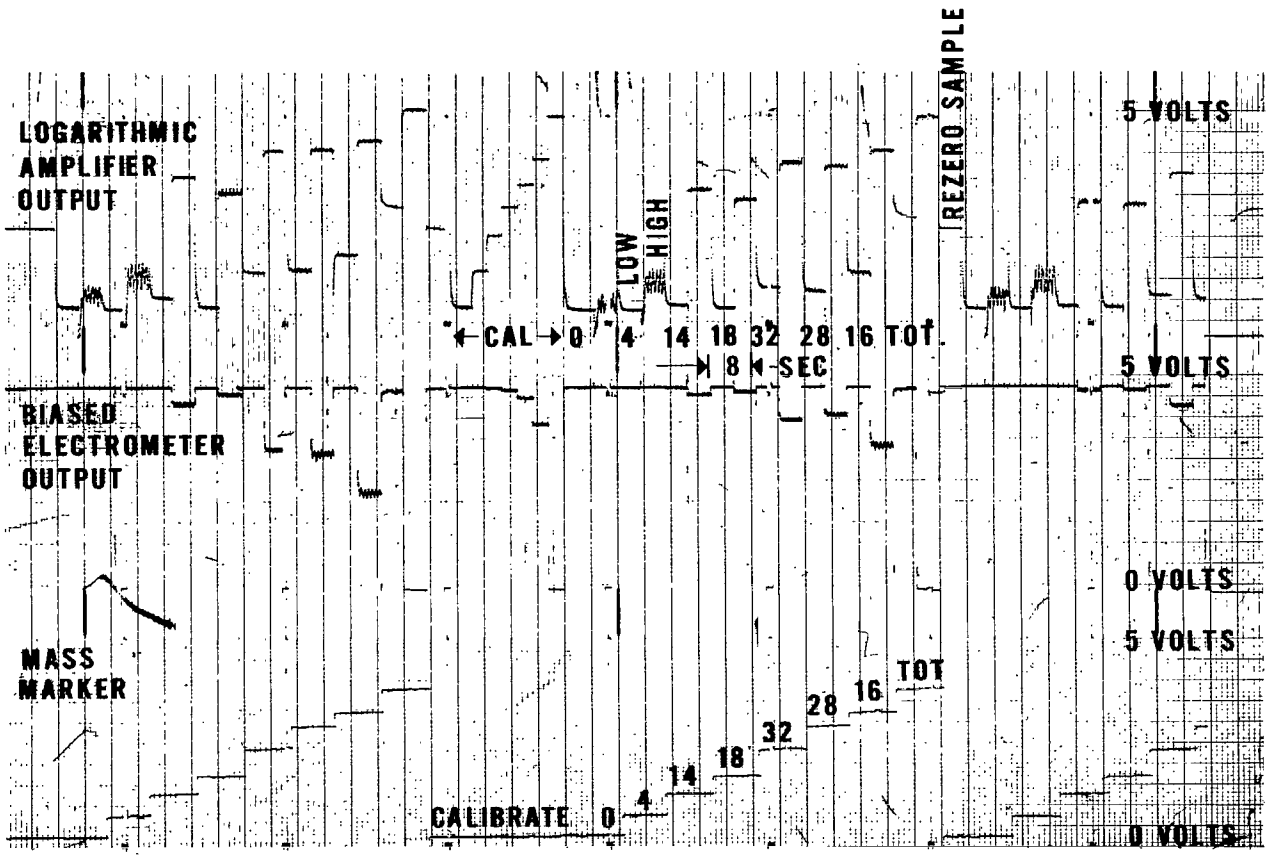

Figure 14—Photograph of a recording of flight data, showing the format in which the data were received.

Power Supplies

In addition to the electronics discussed above, power supplies convert the 9.3 volts from the supply batteries into the highly regulated voltages required for the operation of the magnetic amplifier, the electrometer, and the spectrometer tube. The spectrometer system required about 26 watts from the batteries.

SYSTEM PERFORMANCE

Enviromental Testing

Extensive tests are carried out on all satellite-borne instruments to simulate both the launch and the orbital environments. Thus, the entire system must be able to withstand accelerations of 20 g's and a vibration spectrum of 5 to 5000 cycles per second at levels from 2.3 to 54 g's. The electronics are also tested at temperatures between -10°C and +50°C.

Calibration

Each spectrometer tube-amplifier combination is tested and calibrated as a unit at least twice, once prior to environmental testing and once after the environmental testing is complete. The procedure is to fine tune the tube by scanning, to check peak shapes and positions for each mass collector, and then to run a complete system calibration with all of the flight electronics using helium, nitrogen and oxygen gases. At this point the tube-amplifier combination is taken off the vacuum system and subjected to the vibration tests. The tube is then put back on the vacuum system and a recheck of the tuning is made. If these scans are in agreement with the previous scans, the spectrometer tube is baked out at 360°C to reduce the background pressure and then another complete calibration is run on the entire system. All calibrations are run using at least two different Veeco RG-1A ionization gages as references. The ionization gages are periodically checked against each other for consistency and generally agree in all respects within about 4% (±2%), except possibly in the system background pressure read by each gage. The absolute calibration for the ion gages is ultimately a laboratory standard McCleod gage.

Flight

The Explorer XVII satellite went into orbit at approximately 2115 EST on April 2, 1963. A typical segment of the telemetry record is shown in Figure 14. The reporting in detail of the flight data will be the subject of a later paper.

ACKNOWLEDGMENTS

The authors are indebted to E. I. Meadows Reed, who initiated the project, for many constructive discussions during the development of this instrument. We are pleased to acknowledge the considerable contributions of P. F. Howden who designed the principal parts of the electronics, particularly the electrometer and logarithmic amplifiers, and of T. F. Iwasaki who guided the development through several difficult phases.

(Manuscript received May 3, 1965)

REFERENCES

1. Townsend, J. W., Jr., Meadows, E. B., and Pressly, E. C., "A Mass Spectrometric Study of the Upper Atmosphere," in: *Rocket Exploration of the Upper Atmosphere,* ed. by R. L. F. Boyd and M. J. Seaton, London: Pergamon Press Ltd., 1954, pp. 169-188.
2. Berry, C. E., "Effects of Initial Energies on Mass Spectra," *Phys. Rev.* 78:597-605, June 1, 1950.
3. Hintenberger, H., and König, L. A., "Mass Spectrometers and Mass Spectrographs Corrected for Image Defects," *Advances in Mass Spectrometry:* ed. by J. D. Waldon, London: Pergamon Press Ltd., 1959, pp. 16-35.

4. Klemperer, O., *"Electron Optics,"* 2d ed., Cambrideg: University Press, 1953, p. 172.

5. Herzog, R. F., "Calculation of Stray Field of a Condenser, the Field being Limited by a Disc," *Zeit. Phys.*, 97(9-10):596-602, November 12, 1935.

6. Herb, R. G., Snowdon, S. C., and Sala, O., "Absolute Voltage Determination of Three Nuclear Reactions", *Phys. Rev.*, 75:246-259, January 15, 1959.

7. Herzog, R. F., "New Information on the Electron-Optical Properties of Magnetic Prisms," *Acta Phys. Austriaca*, 4(4):431-444, 1951 (In German).

8. Camac, M., "Double Focusing with Wedge-Shaped Magnetic Fields", *Rev. Sci. Instrum.*, 22:197-204, March, 1951.

9. Benton, H. B., "Small Lightweight Ionization Gauge Control Circuit", *Rev. Sc. Instrum.*, 30(10): 887-888, October, 1959.

"The aeronautical and space activities of the United States shall be conducted so as to contribute . . . to the expansion of human knowledge of phenomena in the atmosphere and space. The Administration shall provide for the widest practicable and appropriate dissemination of information concerning its activities and the results thereof."

—NATIONAL AERONAUTICS AND SPACE ACT OF 1958

NASA SCIENTIFIC AND TECHNICAL PUBLICATIONS

TECHNICAL REPORTS: Scientific and technical information considered important, complete, and a lasting contribution to existing knowledge.

TECHNICAL NOTES: Information less broad in scope but nevertheless of importance as a contribution to existing knowledge.

TECHNICAL MEMORANDUMS: Information receiving limited distribution because of preliminary data, security classification, or other reasons.

CONTRACTOR REPORTS: Technical information generated in connection with a NASA contract or grant and released under NASA auspices.

TECHNICAL TRANSLATIONS: Information published in a foreign language considered to merit NASA distribution in English.

TECHNICAL REPRINTS: Information derived from NASA activities and initially published in the form of journal articles.

SPECIAL PUBLICATIONS: Information derived from or of value to NASA activities but not necessarily reporting the results of individual NASA-programmed scientific efforts. Publications include conference proceedings, monographs, data compilations, handbooks, sourcebooks, and special bibliographies.

Details on the availability of these publications may be obtained from:

SCIENTIFIC AND TECHNICAL INFORMATION DIVISION

NATIONAL AERONAUTICS AND SPACE ADMINISTRATION

Washington, D.C. 20546